International Journal of Impact Engineering 94 (2016) 1–12

Contents lists available at ScienceDirect

International Journal of Impact Engineering

journal homepage: www.elsevier.com/locate/ijimpeng

Study on the penetration performance of concept projectile for high-speed penetration (CPHP)

L.L. He [a], X.W. Chen [a,*], Z.H. Wang [b]

[a] Institute of Systems Engineering, China Academy of Engineering Physics, P.O. Box 919-401, Mianyang, 621999 Sichuan, China
[b] Taiyuan University of Technology, Taiyuan, 030024 Shanxi, China

ARTICLE INFO

Article history:
Received 2 June 2015
Received in revised form 6 March 2016
Accepted 18 March 2016
Available online 22 March 2016

Keywords:
CPHP
DOP
Mass loss
HAZ
Shape variation

ABSTRACT

Two-group penetration tests of Concept Projectile for High-speed Penetration (CPHP) are carried out with striking velocity ranging from 1130 m/s to 1650 m/s. Almost all projectiles are integral after penetration except the one at striking velocity 1650 m/s. The maximum dimensionless Depth of Penetration (DOP) reaches 78.9 at striking velocity 1415 m/s with the concrete strength as 33.4 MPa. It further confirms that CPHP has excellent structural stability and penetration performance into concrete target at high striking velocities. The penetration performances of CPHP made of different materials are also compared. It indicates that the strength and ductility of material jointly control the penetration performance of CPHP. The mass loss of CPHP distributes not only in its nose but also in its shank. The CPHP nose still keeps ogival and the surface of CPHP shank recedes inward. Furthermore, the mass loss mechanism is studied by metallographic observation. It indicates that the heat transformed from frictional work between target and projectile is the main cause of Heat Affected Zone (HAZ), and the peeling of molten surface layer is the main cause of mass loss. Several White Narrow Bands (WNBs) in CPHP nose tip contribute minor mass loss due to its rare number and limited dimensions. Finally, the analytical model for DOP of CPHP was derived. The model prediction is validated by the available experimental result.

1. Introduction

Earth Penetration Weapon (EPW) penetrates into the underground fortifications to produce massive destruction to the structure and especially to the personnel and equipment inside. In order to insure the damage efficiency of EPW, the penetrator structure should be kept integral until the prospective Depth of Penetration (DOP) is achieved. However, the buried depth of the underground fortifications significantly increases nowadays. Correspondingly, the DOP of EPW should be dramatically increased. This becomes a great challenge for the design of the structure of EPW. It should be noted that only normal penetration is considered in the present manuscript, since this gesture is the most effective way for penetration.

Commonly, increasing the kinetic energy of projectile per unit cross section area is the effective way to increase the DOP of projectile. For given projectile mass, the larger the aspect ratio and the higher the striking velocity, the deeper the DOP of projectile could theoretically achieve. In reality, both of them could not be raised indefinitely, since the projectile structure may go unstable, and the bending, buckling or other mode of failure may occur easily with large aspect ratio and high striking velocities. The trade-off between geometry and striking velocity of projectile should be achieved in order to obtain the best penetration performance.

It is easy to find studies on the projectile with ogival nose and cylindrical shank. We call this kind of projectile as ogive long-rod projectile. Its aspect ratio is between 6 and 10, and its striking velocity could be as high as about 1000 m/s [1,2]. Nevertheless, when the striking velocity is further raised to the range between 1000 m/s and 1500 m/s, the projectile is inclined to bend or even fail, which would dramatically decrease its penetration performance [3–5].

In this scenario, Erengil and Cargile [6] designed a new type of projectile for high-speed penetration, as shown in Fig. 1. The projectile has ogival nose and circular-truncated-cone shank. The half taper angle of the shank is around 2°. In order to reduce the contact area between projectile shank and target, six grooves are distributed evenly in the shank. Each groove is cut by a semi-cylinder. The cutting line is the generatrix of the semi-cylinder which is parallel to the projectile axis. In this way, the geometry of the projectile shank could be depicted as a cylinder inside and six heaves attached outside. Compared to the ogive long-rod projectile, the heaves play the role as reinforcing bars, which could prevent projectile from bending or buckling during high-speed penetration. Moreover, the comminuted target material could be dispelled from the six grooves. Commonly, this type of projectile is indicated as the Concept Projectile for High-speed Penetration (CPHP).

* Corresponding author. Institute of Systems Engineering, China Academy of Engineering Physics, P.O. Box 919-401, Mianyang, Sichuan 621999, China. Tel.: +86 816 2484336; Fax: +86 816 2281485.
E-mail address: chenxiaoweintu@yahoo.com (X.W. Chen).

http://dx.doi.org/10.1016/j.ijimpeng.2016.03.010

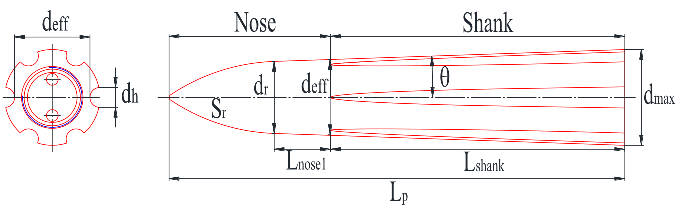

Fig. 1. Scheme of CPHP.

Table 2
Mechanical properties of different high-strength alloy steel.

Materials	$\sigma_{0.2}$ (MPa)	σ_b (MPa)	δ_5 (%)	ψ_c (%)	K_{IC} (MPa·m$^{1/2}$)	α_{KU} (J/cm^2)
DT300(A)	1500	1810	15	50	140	100
G50(B)	1440	1790	14	51	149	68
D6AC(C)	1540	1940	10	34	74	42
AerMet100(D)	1620	1930	10	55	105	–

By contrastive penetration tests, Liang et al. [7] compared the penetration performance of CPHP made of different high-strength alloy steels. They concluded that DT300 is more appropriate for the projectile material than steels G50 and D6AC. Wu et al. [8] stated that CPHP has better structural stability than the ogive long-rod projectile at striking velocities between 800 m/s and 1100 m/s. Erengil and Cargile [6] testified that the CPHP made of AerMet100 is kept integral after penetration into concrete target with unconfined compressive strength of 50 MPa even at striking velocities between 1211 m/s and 1452 m/s. The maximum dimensionless DOP reaches 60 [6]. The available experimental results preliminarily prove the excellent structural stability and penetration capability of CPHP at high striking velocities. More penetration tests should be carried out to enhance this conclusion.

In the present manuscript, two-group penetration tests are carried out for CPHP into unreinforced segmented concrete targets. The striking velocity expands from 1130 m/s to 1650 m/s. The shape variation and mass loss mechanism of CPHP are particularly investigated. Furthermore, the analytical model for the ultimate DOP of CPHP is derived. The model prediction is validated by the available experimental result.

2. Set-up of penetration experiments

2.1. Projectiles

CPHP is adopted in the penetration tests. In order to specifically illustrate the geometry of the projectile, the corresponding characteristic parameters are labeled in Fig. 1. The total length of projectile is L_p. It is divided into nose and shank by the cross section where the groove initiates. The diameter of the cross section is d_{eff}. The aspect ratio of the projectile is defined as L_p/d_{eff}. The nose is comprised of a partial ogive and a small truncated cone. The radius of the ogival generatrix is S_r. The length and minimum diameter of the cone are respectively L_{nose1} and d_r. The Caliber Radius Head (CRH) is approximately defined as $\psi = \psi S_r/d_r$. The shank is a truncated cone with a small half taper angle θ. Its length and maximum diameter are L_{shank} and d_{max}, respectively. Six grooves are cut by six semi-cylinders, whose diameter is d_h. All these above characteristic parameters as well as the mass and material of projectile are listed in Table 1. Specially, Groups I and II indicate the penetration tests carried out in the present manuscript. Groups III and IV refer to the tests in the Ref. [7]. Groups V and VI are the experiments in the Ref. [6]. The mechanical properties of related alloy steels are listed in Table 2, including the yield strength $\sigma_{0.2}$, fracture strength σ_b, elongation percentage δ_5, contraction of cross-section area ψ_c, fracture toughness K_{IC} and impact toughness α_{KU}.

2.2. Targets

The segmented unreinforced concrete target is employed in Groups I and II. For Group I, the target is comprised of three concrete cylinders with equal intervals, as shown in Fig. 2a. For three tests in Group I, the intervals are respectively 300 mm, 300 mm and 1000 mm. Each cylinder is wrapped by iron sheet with thickness of 2 mm. For Group II, two cylinders are welded together and 5 mm iron sheet is wrapped outside the concrete cylinder, as shown in Fig. 2b. Other properties of targets are listed in Table 1, including the diameter d_{ti} (i = 1,2,3), length H_{ti} (i = 1,2,3), unconfined compressive strength f_c and density ρ_t of concrete target as well as the material, Moh's hardness H and average diameter d_a of the aggregate in concrete target. The properties of target in Groups III–VI [6,7] are also listed in Table 1. The targets are fixed with sand bags and wooden chocks during penetration.

2.3. Experimental layout

The plan view of the experimental layout of Group I is shown in Fig. 3. The CPHP was launched by 100 mm-caliber smooth-bore powder gun. The projectiles were fitted with sabots and obturators that separated from the projectiles prior to impact. The free flying velocity of CPHP is measured by the break screens and high-speed photography camera. The flying and impact gesture of CPHP is recorded by the high-speed photography camera. Sabot stopping device is placed in front of the target to avoid the secondary

Table 1
Properties of CPHP and unreinforced concrete target in six groups.

CPHP													
Group no.	Material	M_0 (kg)	d_r (mm)	S_r (mm)	$\psi = S_r/d_r$	L_{nose1} (mm)	d_{max} (mm)	d_h (mm)	θ (°)	L_{shank} (mm)	d_{eff} (mm)	L_p (mm)	L_p/d_{eff}
I/II	DT300(A)	1.83	36.0	101	3	28.4	48.0	10.0	1.7	148.4	38.0	230.2	6.0
III	DT300/G50(B)/D6AC(C)	0.44	21.9	66	3	30.8	30.0	6.0	1.7	89.0	24.0	153.3	6.4
IV	DT300	1.43	32.9	99	3	31.7	45.0	10.0	1.7	147.9	35.0	230.2	6.6
V/VI	AerMet100(D)	1.43	32.9	99	3	27.4	45.2	10.5	2.0	152.4	34.5	231.1	6.7
Unreinforced concrete target													
Group no.	Type	$d_{t1} \times H_{t1}$ (mm × mm)		$d_{t2} \times H_{t2}$ (mm × mm)		$d_{t3} \times H_{t3}$ (mm × mm)		f_c (MPa)	ρ_t (kg/m^3)		d_a (mm)	Aggregate material/H	
I	Segmented	1000 × 600		1000 × 600		800 × 1050		48.0	2350		8	Limestone/3	
II	Segmented	1000 × 1200		1000 × 1200		–		33.4	2400		5	Limestone/3	
III	Monolithic	800 × 1050		–		–		48.0	2350		8	Limestone/3	
IV	Segmented	800 × 1050		800 × 1050		–		48.0	2350		8	Limestone/3	
V	Monolithic	1370 × 1900		–		–		50.0	–		–	–	
VI	Segmented	1370 × 1000		1830 × 1830		–		50.0	–		–	–	